31st Annual International Conference of the IEEE EMBS
Minneapolis, Minnesota, USA, September 2-6, 2009

Shearwave Dispersion Ultrasound Vibrometry Applied to *In Vivo* Myocardium

Cristina Pislaru, Matthew W. Urban, *Member, IEEE*, Ivan Nenadic, and James F. Greenleaf, *Life Fellow, IEEE*

Abstract— **Diastolic properties of the myocardium are important for normal cardiac function and may contribute to the condition of heart failure. Measuring the viscoelastic properties of the left ventricular myocardium is difficult in vivo using noninvasive methods. In this study, we used a mechanical actuator to create harmonic, propagating mechanical waves in the myocardial tissue in vivo. The motion was measured using ultrasound imaging techniques. The wave propagation velocities were measured over the 50-350Hz frequency range. The dispersion curves were fit with an asymmetrical Lamb wave model to obtain estimates of the shear elasticity and viscosity of the myocardial tissue. The method was applied to estimate viscoelastic properties of the myocardium during diastole and systole.**

I. Introduction

DIASTOLIC dysfunction is the impaired ability of the heart to fill and maintain its stroke volume at physiologic filling pressures. Isolated diastolic dysfunction is common, especially in the elderly. Up to 40% of heart failure patients have normal ejection fraction, and some of these patients have abnormal diastolic properties of the myocardium [1,2,3,4]. Common causes of diastolic dysfunction are abnormal left ventricular relaxation [2] and increased left ventricular chamber stiffness [2, 3]. Knowledge of the quantitative values of the viscoelastic properties of the myocardium would greatly improve the clinician's ability to evaluate diastolic dysfunction in an individual patient.

Several investigators have attempted to make measurements of the fundamental mechanical properties of the myocardium using invasive and noninvasive methods [2, 4, 5]. More recent noninvasive methods include tagged magnetic resonance imaging, tissue Doppler imaging, strain and strain rate echocardiography, mechanical wave imaging, and acoustic radiation force impulse imaging [6-13]

In this paper, we present a method called Shearwave Dispersion Ultrasound Vibrometry (SDUV) which measures the change in shear wave velocity with frequency [14, 15]. This characteristic is then fit with a model for the asymmetrical Lamb wave to assess the viscoelastic properties of the tissue, as previously tested in excised myocardial slabs [16]. We present results from *in vivo* tests in open-chest experiments with pigs.

This work was supported in part by grant EB002167 from the National Institutes of Health.

The authors are with the Department of Physiology and Biomedical Engineering, Mayo Clinic College of Medicine, Rochester, MN 55905 USA (Contact information for M. W. Urban: phone: 507-538-1522; fax: 507-266-0361; e-mail: urban.matthew@mayo.edu).

II. Methods

A. Dispersion Ultrasound Vibrometry

Chen, *et al*., have developed a method using ultrasound radiation force and the measurement of the dispersion of shear wave velocities to estimate the shear elasticity and viscosity of soft tissue-like materials [14]. This work was been extended to create the SDUV method to make it compatible with current ultrasound scanners by employing repeated ultrasound tonebursts to obtain motion that has multiple frequency components at which the shear wave velocities can be measured and dispersion can be evaluated [15].

B. Asymmetrical Lamb Wave Model

An asymmetrical Lamb wave model was developed by Kanai [17]. He modeled the heart wall as a viscoelastic plate with thickness $2h$ based on the Voigt model. Assuming that the shear modulus, μ, is much smaller than the bulk modulus, λ, he arrived at the following equation

$$f(c_L, \mu, \omega) = 4k_L^3 \cosh(k_L h)\sinh(\beta h) - \left(2k_L^2 - k_s^2\right)^2 \sinh(k_L h)\cosh(\beta h) - k_s^4 \cosh(k_L h)\cosh(\beta h) = 0, \quad (1)$$

where c_L is the Lamb wave velocity, $k_L = \omega/c_L(\mu, \omega)$, $\beta = \sqrt{k_L^2 - k_s^2}$, $k_s = \omega\sqrt{\rho_m/\mu}$, ρ_m is myocardial density, and $\mu = \mu_1 + i\omega\mu_2$ where μ_1 and μ_2 are the shear elasticity and viscosity, respectively. The measured shear wave velocities are then fit with (1) to extract μ_1 and μ_2.

C. Experiment

An open-chest protocol was used as approved by our Institutional Animal Care and Use Committee. Using the principles of SDUV, we designed an experiment that used a mechanical shaker with a 6 mm diameter ball bearing attached to a rod to induce motion into the heart wall. The shaker (V203, Ling Dynamic Systems Limited, Hertfordshire, UK) was driven with a signal generator (33120A, Agilent, Santa Clara, CA) and an amplifier (XLS 202, Crown Audio, Inc., Elkhart, IN). The motion was measured using a high frame rate acquisition sequence using an Ultrasonix Sonix RP system (Sonix RP, Ultrasonix Medical Corporation, Richmond, BC, Canada). The motion

was captured using an M-mode type scheme with multiple lines, separated by 0.9 mm. Frame rates were on the order of ~2500 Hz. The linear array transducer was first wrapped in a latex cover filled with ultrasound gel, then another cover filled with water to provide a stand-off. The rod attached to the shaker was centered in the B-mode imaging plane and the sequence was defined to measure waves propagating along the length of the array. The rod was positioned on the mid-anterior left ventricular wall. Care was taken to avoid obstructing the main coronary arteries and branches.

Radiofrequency (RF) data were acquired for 3 seconds of vibration to capture multiple heart cycles. The initiation of the vibration and data acquisition was gated on the electrocardiographic (ECG) R-wave. The data were saved and processed offline using cross-spectral analysis and Kalman filtering to obtain motion and phase of the vibration for discrete segments in space and time [18, 19]. The phase was plotted versus distance of propagation and a linear regression was performed to find the phase velocity using $c = \omega \Delta r / \Delta \phi$, where Δr is the distance and $\Delta \phi$ is the phase difference. The phase velocities over the 50-350 Hz range were plotted and μ_1 and μ_2 estimated by fitting the data with equation 1.

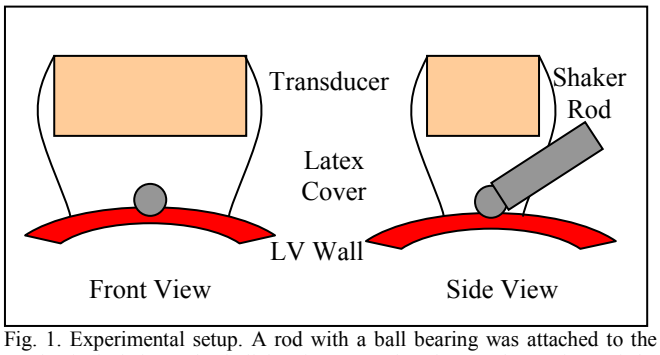

Fig. 1. Experimental setup. A rod with a ball bearing was attached to the mechanical shaker. The ball bearing was placed onto the surface of the myocardial wall. A linear array transducer was suspended above the heart wall and coupled with a water-filled latex cover.

III. Results

Figure 2 shows one sample M-mode image of a three second acquisition while inducing vibration at 100 Hz. The vibration was observed from the M-mode data. To isolate the heart wall, manual segmentation was performed by drawing boundaries for the epicardial (outer) and endocardial (inner) surfaces (shown as red lines in Fig. 2).

Figures 3 and 4 show the displacement amplitude and phase at four different lateral locations in the myocardium. The displacement has a unique spatiotemporal distribution and decreases as the distance from the shaker increases. A median filter with a kernel size of 3 x 1 was used to filter the phase data to exclude outliers and smooth the data for calculation of the phase velocities. The phase is fairly consistent throughout the thickness of the myocardium, indicating that the heart wall is vibrating in phase.

Figure 5 shows the phase velocity at 100 Hz through the heart cycle. In Fig. 5(a) the spatiotemporal distribution of the phase velocity is shown, while in Figure 3(b) a median was taken for each time point over the thickness of the myocardium. The heart is at the beginning of systole at $t = 0$ ms and then proceeds to diastole from about $t = 400$-800 ms. The phase velocity is almost a binary function through time, having one value during systole and a lower value during diastole. There is a somewhat gradual decline from the peak value during systole to the baseline value during diastole. The pattern is very consistent for different heart cycles.

Figure 6 shows the phase velocity average through time for frequencies 50-350 Hz. The open circles are the mean of 3-5 repeated acquisitions. The curves are less well defined at higher frequencies, probably because of lower motion amplitudes, which lead to less reliable phase and phase velocity estimates. However, the binary nature from systole to diastole is maintained.

We averaged the phase velocities during systole and diastole for the frequencies of interest and the results are shown in Fig. 7. We used the Lamb wave model in (1) to estimate the viscoelastic properties using the mean values of the phase velocities, and found μ_1 = 1.7 kPa and μ_2 = 3.2 Pa·s for diastole, and μ_1 = 31.0 kPa and μ_2 = 5.0 Pa·s. The shear elasticity increased by a factor of over 18, and the shear viscosity increased by a factor of 1.5 from diastole to systole.

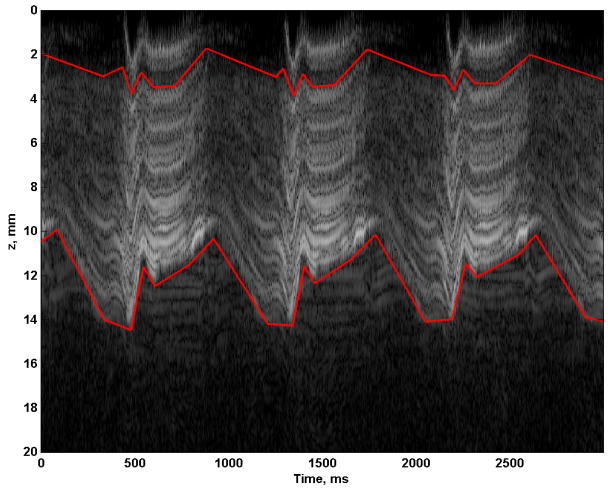

Fig. 2. M-mode and manually drawn mask borders for subsequent analysis of displacement amplitude and phase and phase velocity.

IV. Discussion

The results from this SDUV experiment indicate that the phase velocities and the viscoelastic material properties can be measured by SDUV method *in vivo*. These properties change during the heart cycle, as expected. During diastole, the heart muscle is relaxed and the passive characteristics of the tissue are dominant. During systole, the contractile elements are activated and myofibers shorten (wall thickens), and their effect dominate the characteristics of the tissue disclosed by an increase in shear elasticity and viscosity.

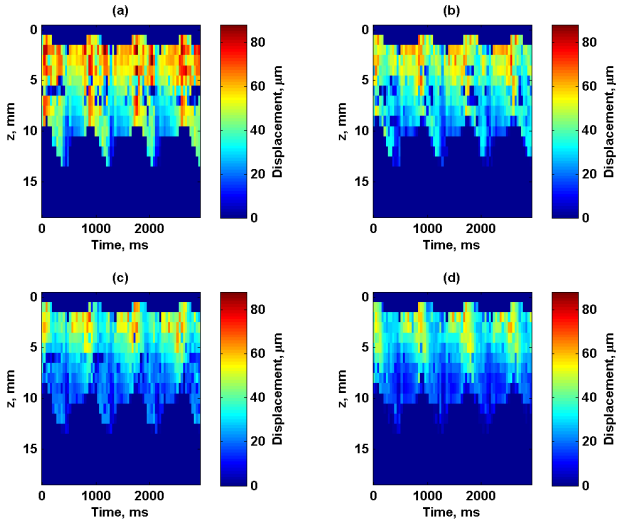

Fig. 3. Displacement amplitude through heart cycle at 100 Hz at different lateral locations from the shaker excitation point. (a) x = 0 mm, (b) x = 1.8 mm, (c) x = 3.6 mm, (d) x = 5.4 mm.

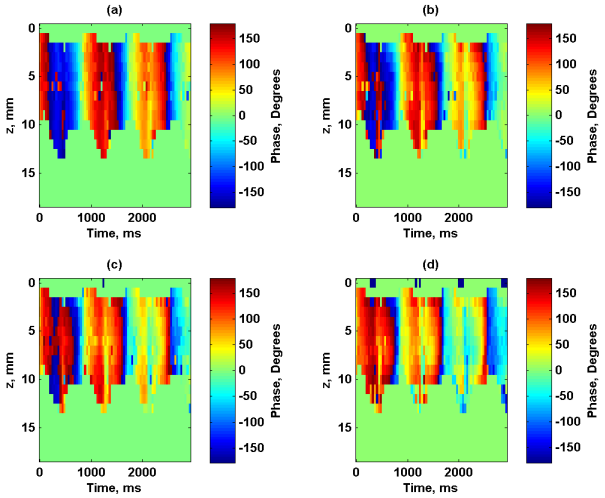

Fig. 4. Displacement phase through heart cycle at 100 Hz at different lateral locations from the shaker excitation point. (a) x = 0 mm, (b) x = 1.8 mm, (c) x = 3.6 mm, (d) x = 5.4 mm.

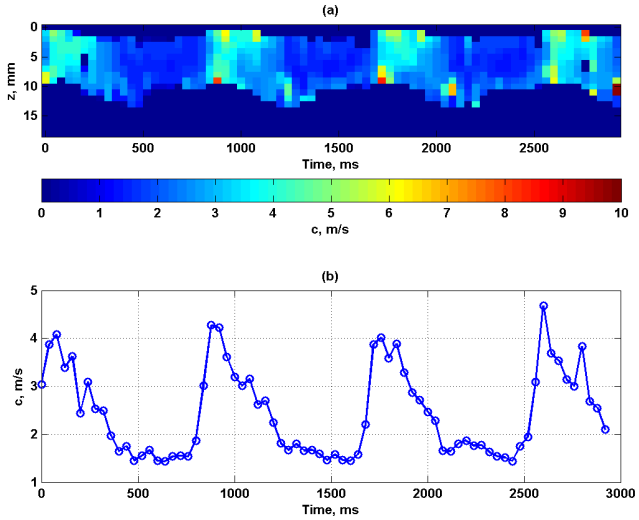

Fig. 5. Phase velocity through heart cycle at 100 Hz. (a) Spatiotemporal distribution of phase velocity, (b) Median value through thickness at each time point.

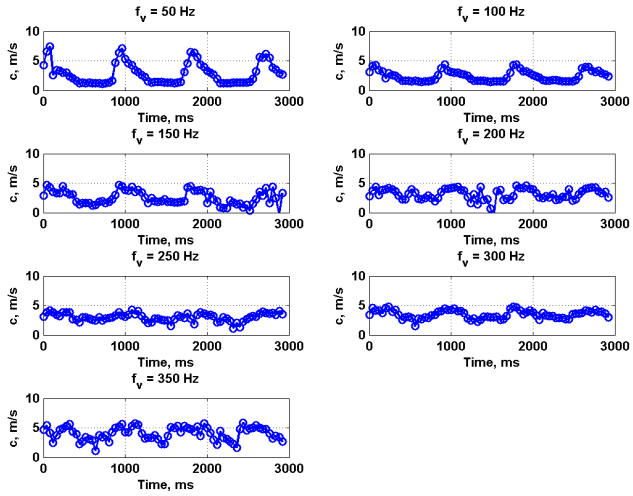

Fig. 6. Phase velocity through heart cycle at frequencies 50-350 Hz averaged over five acquisitions.

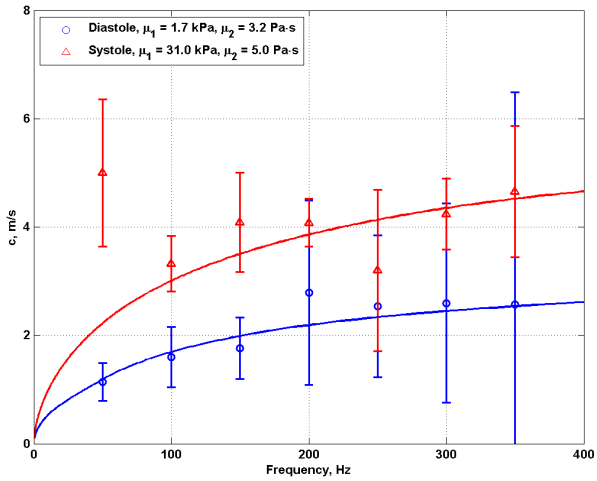

Fig. 7. Phase velocity dispersion in systole and diastole averaged over five acquisitions.

Application of the Lamb wave model seemed appropriate. The phase images in Fig. 4 show that the phase is conserved through the thickness of the myocardium indicating that the tissue is moving in unison, which is the characteristic motion of the asymmetric Lamb wave mode. The model fit the data relatively well, consistent with previous results in excised myocardial slabs [16]. The most reliable estimates were obtained during diastole, probably due to the reduced wall motion during this period. In the future, we will pursue curve fitting that weights more the lower frequency phase velocities because of their lower standard deviations.

Our results agree with previous findings. In human myocardium, Kanai has found wave propagation speeds ranging from 1-7 m/s for a frequency range of 20-90 Hz [17]. This range agrees with our results in swine myocardium. Kanai also tabulated measurements of μ_1 and μ_2 in cardiac and other tissues. The values of μ_1 = 24-30 kPa acquired at end-systole in human myocardium agree with μ_1 during systole found in this study. However, their values for μ_2 = 70-400 Pa·s were substantially higher. Further studies

are needed to validate this method *in vivo* and to explain discrepancies with previous results.

In this study we used a mechanical shaker and few assumptions were made. First, we assumed that the induced waves were planar as they propagated along the azimuthal direction of the transducer. There may be some near-field effects due to the size of the actuator rod. This may explain the high value for the 50 Hz component in Fig. 7 for the systolic dispersion curve. A similar effect was reported by Catheline, *et al*. [20] and was attributed to diffraction due to the size of the vibrating rod. Also, we assumed that myocardial wall is homogeneous over the depth measured.

The shaker has a magnitude frequency response that varies with a $1/f$ characteristic and we adjusted the driving voltage to compensate for this response. However, a constant displacement could not be maintained at higher frequencies. The motion was ~10-40 μm, which in most cases was enough for accurate phase estimation. However, during systole, characterized by higher wall motion and stiffness, phase estimation was noisier. Another assumption is that the tissue being measured stayed in the elevational plane of the linear array transducer. Variations could cause measurement of different parts of the propagating waves and bias the phase velocity estimate.

In the future, we will use ultrasound radiation force to excite the tissue and measure the motion with pulse-echo ultrasound with the same linear array transducer. We can then avoid some of the assumptions made here and capture the data for constructing the dispersion curves in one acquisition, in a completely noninvasive approach.

V. Conclusions

We performed an *in vivo* experiment on the left ventricular wall of a swine heart in which we measured the dispersive phase velocity of Lamb waves using a mechanical shaker as the excitation source. The phase was consistent through the thickness of the myocardium, confirming asymmetric Lamb wave modal behavior. We fit a Lamb wave model to the dispersion curves and estimated shear elasticity and viscosity for the heart wall during systole and diastole. Future work will include the use of ultrasound radiation force as the excitation source to characterize the phase velocity dispersion.

Acknowledgment

The authors are grateful to Randall Kinnick and Jill Anderson for animal experiment support, Thomas Kinter for computer support, Jennifer Milliken for administrative support, and Kris Dickie and Reza Zahiri at Ultrasonix Medical Corporation for technical support.

References

[1] W. H. Gaasch and M. R. Zile, "Left ventricular diastolic dysfunction and diastolic heart failure," *Annu. Rev. Med.,* vol. 55, pp. 373-394, 2004.

[2] M. R. Zile, C. F. Baicu, and W. H. Gaasch, "Diastolic heart failure - Abnormalities in active relaxation and passive stiffness of the left ventricle," *N. Engl. J. Med.,* vol. 350, pp. 1953-1959, May 2004.

[3] M. R. Zile and D. L. Brutsaert, "New concepts in diastolic dysfunction and diastolic heart failure: Part I: diagnosis, prognosis, and measurements of diastolic function," *Circulation,* vol. 105, pp. 1387-1393, 2002.

[4] A. Borbely, J. van der Velden, Z. Papp, J. G. F. Bronzwaer, I. Edes, G. J. M. Stienen, and W. J. Paulus, "Cardiomyocyte stiffness in Diastolic heart failure," *Circulation,* vol. 111, pp. 774-781, Feb 2005.

[5] M. Kawaguchi, I. Hay, B. Fetics, and D. A. Kass, "Combined ventricular systolic and arterial stiffening in patients with heart failure and preserved ejection fraction - Implications for systolic and diastolic reserve limitations," *Circulation,* vol. 107, pp. 714-720, Feb 2003.

[6] E. A. Zerhouni, D. M. Parish, W. J. Rogers, A. Yang, and E. P. Shapiro, "Human heart: tagging with MR imaging--a method for noninvasive assessment of myocardial motion," *Magn. Reson. Imaging,* vol. 169, pp. 59-63, 1988.

[7] K. Isaaz, "Tissue Doppler imaging for the assessment of left ventricular systolic and diastolic functions," *Curr. Opin. Cardiol.,* vol. 17, pp. 431-442, Sep 2002.

[8] G. R. Sutherland, G. Di Salvo, P. Claus, J. D'Hooge, and B. Bijnens, "Strain and strain rate imaging: a new clinical approach to quantifying regional myocardial function," *J. Am. Soc. Echocardiogr.,* vol. 17, pp. 788-802, 2004.

[9] A. Heimdal, A. Stoylen, H. Torp, and T. Skjaerpe, "Real-time strain rate imaging of the left ventricle by ultrasound," *J. Am. Soc. Echocardiogr.,* vol. 11, pp. 1013-1019, Nov 1998.

[10] C. Pislaru, T. P. Abraham, and M. Belohlavek, "Strain and strain rate echocardiography," *Curr. Opin. Cardiol.,* vol. 17, pp. 443-454, Sep 2002.

[11] C. Pislaru, C. J. Bruce, P. C. Anagnostopoulos, J. L. Allen, J. B. Seward, P. A. Pellikka, E. L. Ritman, and J. F. Greenleaf, "Ultrasound strain imaging of altered myocardial stiffness: stunned versus infarcted reperfused myocardium," *Circulation,* vol. 109, pp. 2905-10, 2004.

[12] M. Pernot, K. Fujikura, S. D. Fung-Kee-Fung, and E. E. Konofagou, "ECG-gated, mechanical and electromechanical wave imaging of cardiovascular tissues in vivo," *Ultrasound Med. Biol.,* vol. 33, pp. 1075-1085, Jul 2007.

[13] S. J. Hsu, R. R. Bouchard, D. M. Dumont, P. D. Wolf, and G. E. Trahey, "In vivo assessment of myocardial stiffness with acoustic radiation force impulse imaging," *Ultrasound Med. Biol.,* vol. 33, pp. 1706-1719, Nov 2007.

[14] S. Chen, M. Fatemi, and J. F. Greenleaf, "Quantifying elasticity and viscosity from measurement of shear wave speed dispersion," *J. Acoust. Soc. Am.,* vol. 115, pp. 2781-5, Jun 2004.

[15] S. Chen, M. W. Urban, C. Pislaru, R. Kinnick, Y. Zheng, A. Yao, and J. F. Greenleaf, "Shearwave dispersion ultrasound vibrometry (SDUV) for measuring tissue elasticity and viscosity," *IEEE Trans. Ultrason. Ferroelectr. Freq. Control,* vol. 56, pp. 55-62, Jan 2009.

[16] I. Nenadic, M. W. Urban, and J. F. Greenleaf, "Study of Lamb wave dispersion in porcine myocardium," *J. Acoust. Soc. Am.,* vol. 124, pp. 2445-2445, 2008.

[17] H. Kanai, "Propagation of spontaneously actuated pulsive vibration in human heart wall and in vivo viscoelasticity estimation," *IEEE Trans Ultrason Ferroelectr Freq Control,* vol. 52, pp. 1931-42, Nov 2005.

[18] H. Hasegawa and H. Kanai, "Improving accuracy in estimation of artery-wall displacement by referring to center frequency of RF echo," *IEEE Trans. Ultrason. Ferroelectr. Freq. Control,* vol. 53, pp. 52-63, Jan 2006.

[19] Y. Zheng, S. Chen, W. Tan, R. Kinnick, and J. F. Greenleaf, "Detection of tissue harmonic motion induced by ultrasonic radiation force using pulse-echo ultrasound and Kalman filter," *IEEE Trans. Ultrason. Ferroelectr. Freq. Control,* vol. 54, pp. 290-300, Feb 2007.

[20] S. Catheline, F. Wu, and M. Fink, "A solution to diffraction biases in sonoelasticity: the acoustic impulse technique," *J Acoust Soc Am,* vol. 105, pp. 2941-50, May 1999.